Molecular Cell, Volume *80*

Supplemental Information

Actionable Cytopathogenic Host Responses of Human Alveolar Type 2 Cells to SARS-CoV-2

Ryan M. Hekman, Adam J. Hume, Raghuveera Kumar Goel, Kristine M. Abo, Jessie Huang, Benjamin C. Blum, Rhiannon B. Werder, Ellen L. Suder, Indranil Paul, Sadhna Phanse, Ahmed Youssef, Konstantinos D. Alysandratos, Dzmitry Padhorny, Sandeep Ojha, Alexandra Mora-Martin, Dmitry Kretov, Peter E.A. Ash, Mamta Verma, Jian Zhao, J.J. Patten, Carlos Villacorta-Martin, Dante Bolzan, Carlos Perea-Resa, Esther Bullitt, Anne Hinds, Andrew Tilston-Lunel, Xaralabos Varelas, Shaghayegh Farhangmehr, Ulrich Braunschweig, Julian H. Kwan, Mark McComb, Avik Basu, Mohsan Saeed, Valentina Perissi, Eric J. Burks, Matthew D. Layne, John H. Connor, Robert Davey, Ji-Xin Cheng, Benjamin L. Wolozin, Benjamin J. Blencowe, Stefan Wuchty, Shawn M. Lyons, Dima Kozakov, Daniel Cifuentes, Michael Blower, Darrell N. Kotton, Andrew A. Wilson, Elke Mühlberger, and Andrew Emili

Supplemental Figure titles.

Figure S1: Related to Figure 1.
Functional annotation and correlation analysis of the (phospho)proteomics data.

Figure S2: Related to Figure 2.
SARS-CoV-2 infected iAT2s show altered cellular processes and phenotype triggered by deregulated phosphorylation events.

Figure S3: Related to Figure 2.
Modelling virus-host protein interactions from iAT2 (phospho)proteomics expression dataset.

Figure S4: Related to Figure 3. (A).
PCA clustering of infected iAT2 phosphoproteomic data and phase-separation analysis of SARS-CoV-2 Nucleoprotein (N).

Figure S5: Related to Figure 4 and 5.
Deregulated cellular processes in SARS-CoV-2 infected iAT2s and comparative analysis of present and published SARS-CoV-2 infection proteomics datasets.

Figure S6: Related to Figure 6.
Drug compound screening of SARS-CoV-2 infected Vero and iAT2 cells.

Figure S7: Related to Figure 2, 3 and 4.
SARS-CoV-2 infected iAT2s show deregulated cell cycle, translation and DNA damage responses.

Supplemental Figures

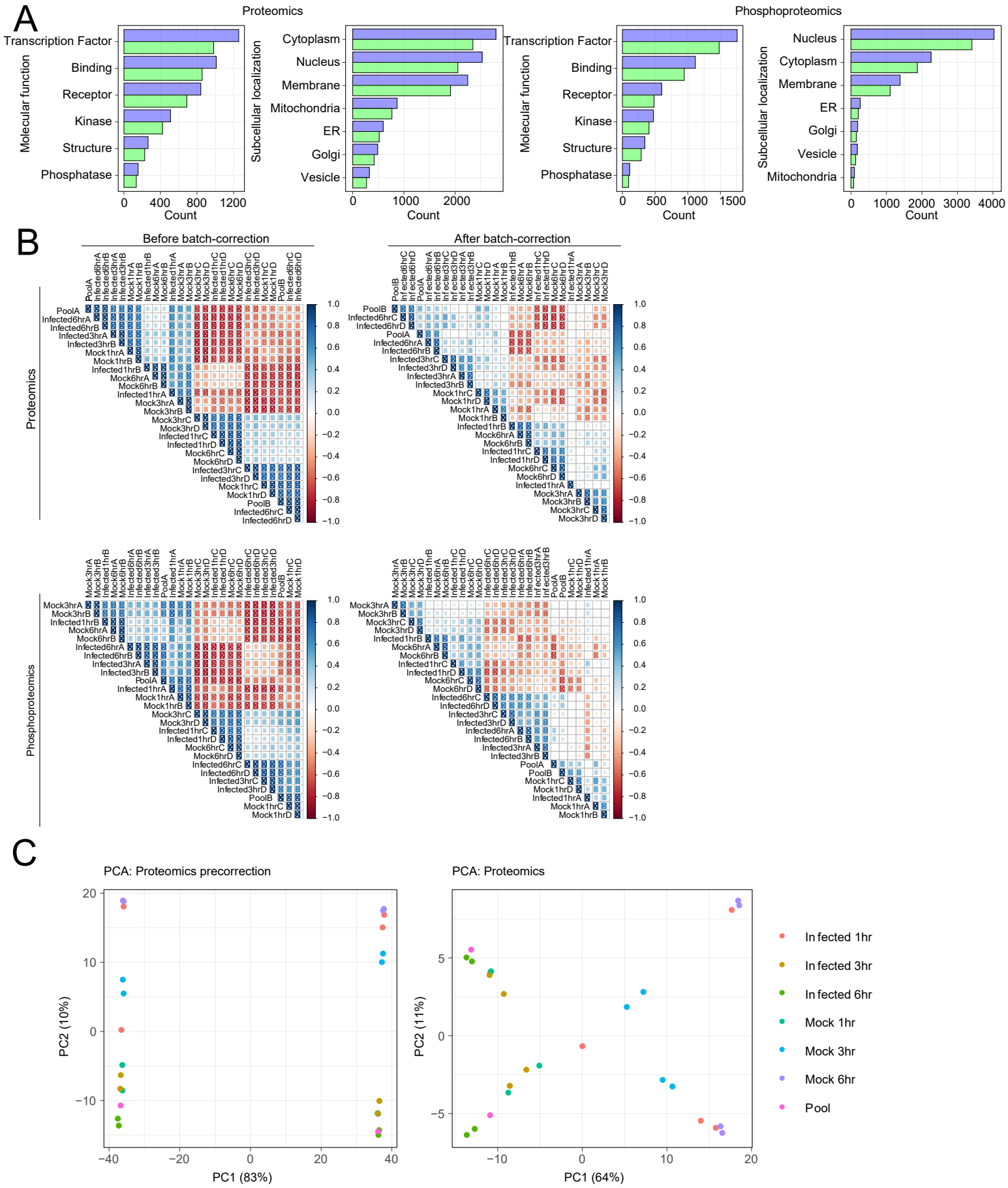

Supplementary Figure S1: Functional annotation and correlation analysis of the (Phospho)proteomics data, Related to Figure 1. (A) Frequency of molecular functions and subcellular localization of proteins and phosphosites from UniProt. Total numbers for the 1, 3 and 6 hpi timeponts shown in blue and differential from UniProt regulated for atleast one timepoint shown in green. (**B)** Correlation plots between samples showing before and after batch correction for the early time point proteomics and phosphoproteomic data, respectively. Replicates A and B were in one set of TM- multiplexed samples and C and D were in a second set. **(C)** Principal component analysis (PCA) of proteomic group reporter ion intensity for log transformed, normalized data showing pre-batch correction (left) and post-batch correction (right).

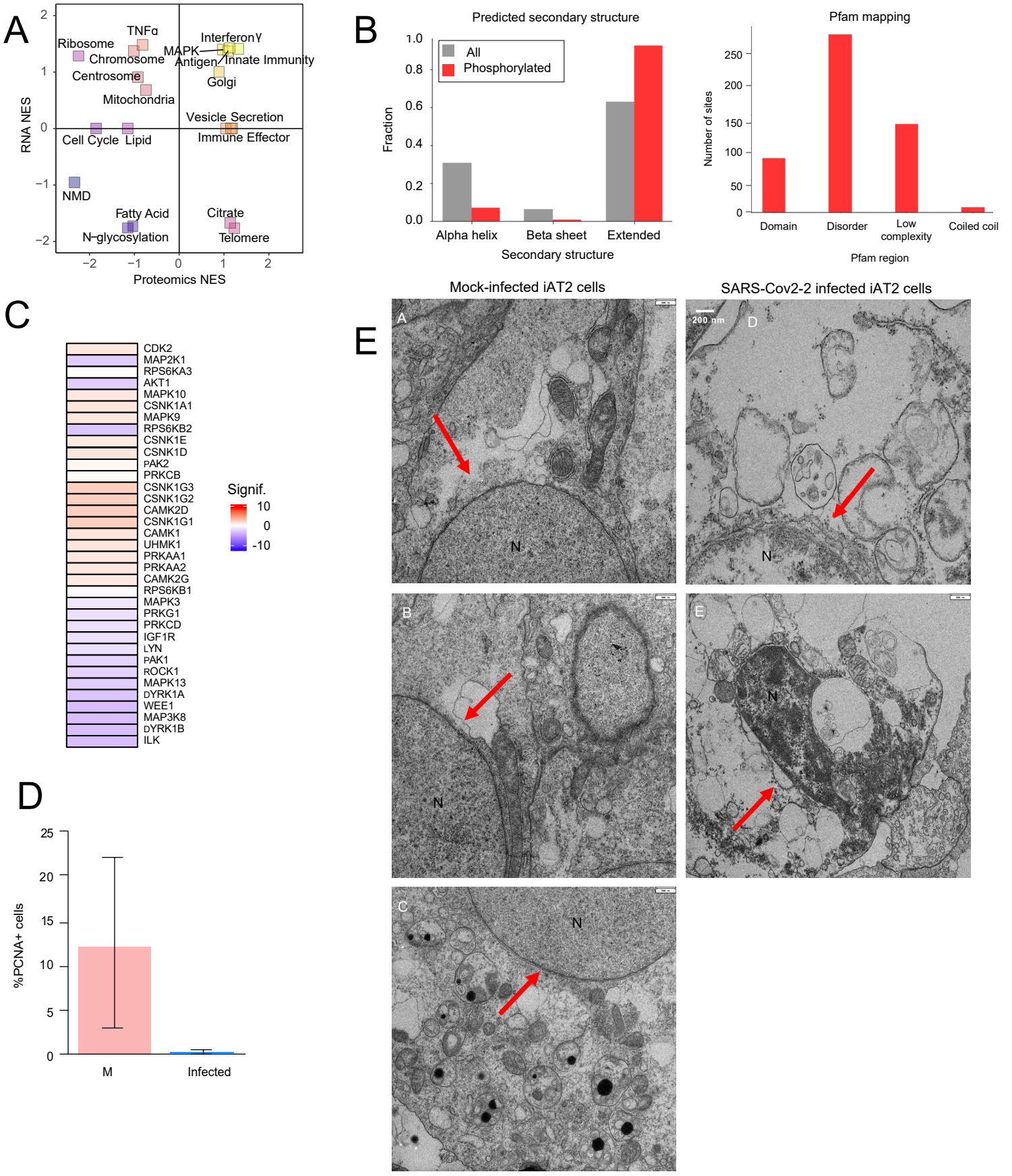

Supplementary Figure S2: SARS-CoV-2 infected iAT2s show altered cellular processes and phenotype triggered by deregulated phosphorylation events, Related to Figure 2. (A). Scatter plot comparing enriched pathways in iAT2s 24 hpi at proteome (this study) versus mRNA level (RNAseq data from Huang et al., 2020); axis shows Normalized Enrichment Score (NES) for the respective data as determined by GSEA, color intensity proportional to summed NES at RNA and protein levels. **(B)**. (Left panel) Predicted 3-state secondary structure distribution for the hyperphosphorylated residues is shown as red bars. The secondary structure for all residues in the same proteins is shown as grey bars. (Right panel) Mapping of hyperphosphorylated residues to Pfam entries. **(C)**. Kinase enrichment (24 hpi). Regulated phosphosites (p-value ≤ 0.05, log fold-change ≥0.25) at 24 hpi were subjected to KEA (https://www.maayanlab.net/KEA2/). **(D)**. iAT2 cells were fixed and immunoprobed with antibodies against SARS-CoV-2 N and PCNA. The number of cells expressing PCNA were quantified and presented as percentage of PCNA+ cells. The error bars represent standard deviation (n=3). **(E).** Transmission electron microscopy showing (A-C) mock-infected iAT2 cells with visible nuclear enveloped double membranes, l amellar bodies (C), and (D-F) infected cells in which increased ER is visible adjacent to the nuclear envelope (D,F) and damaged nuclear envelope.

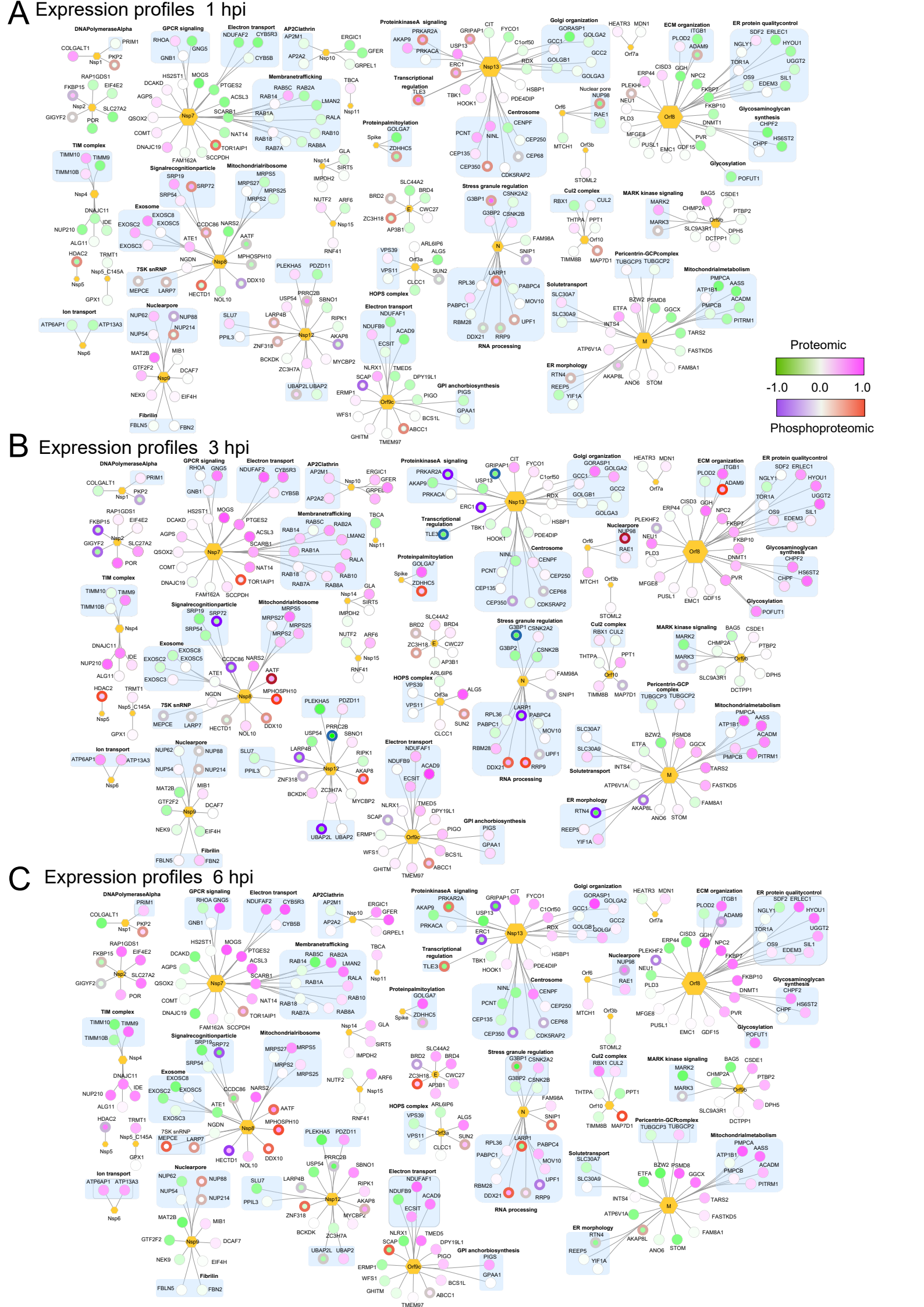
A Expression profiles 1 hpi
B Expression profiles 3 hpi
C Expression profiles 6 hpi
Proteomic
-1.0
0.0
1.0
Phosphoproteomic

Supplementary Figure S3: Modelling virus-host protein interactions from iAT2 (phospho)proteomics expression dataset, Related to Figure 2. (A). Viral-host protein-protein interaction (PPI) sub-network of differentially enriched proteins and phosphoproteins at the 1 hpi, **(B)**. 3 hpi and **(C)** 6 hpi timepoints. Hexagons are viral proteins with size to number of PPI. Circles are the host proteins. Proteins that are more highly expressed in the infected sample as compared to mock are colored and those with lower expression as green. Differentially enriched phosphoproteins are shown with purple - orange border. Functionally grouped proteins are placed within blue rectangles.

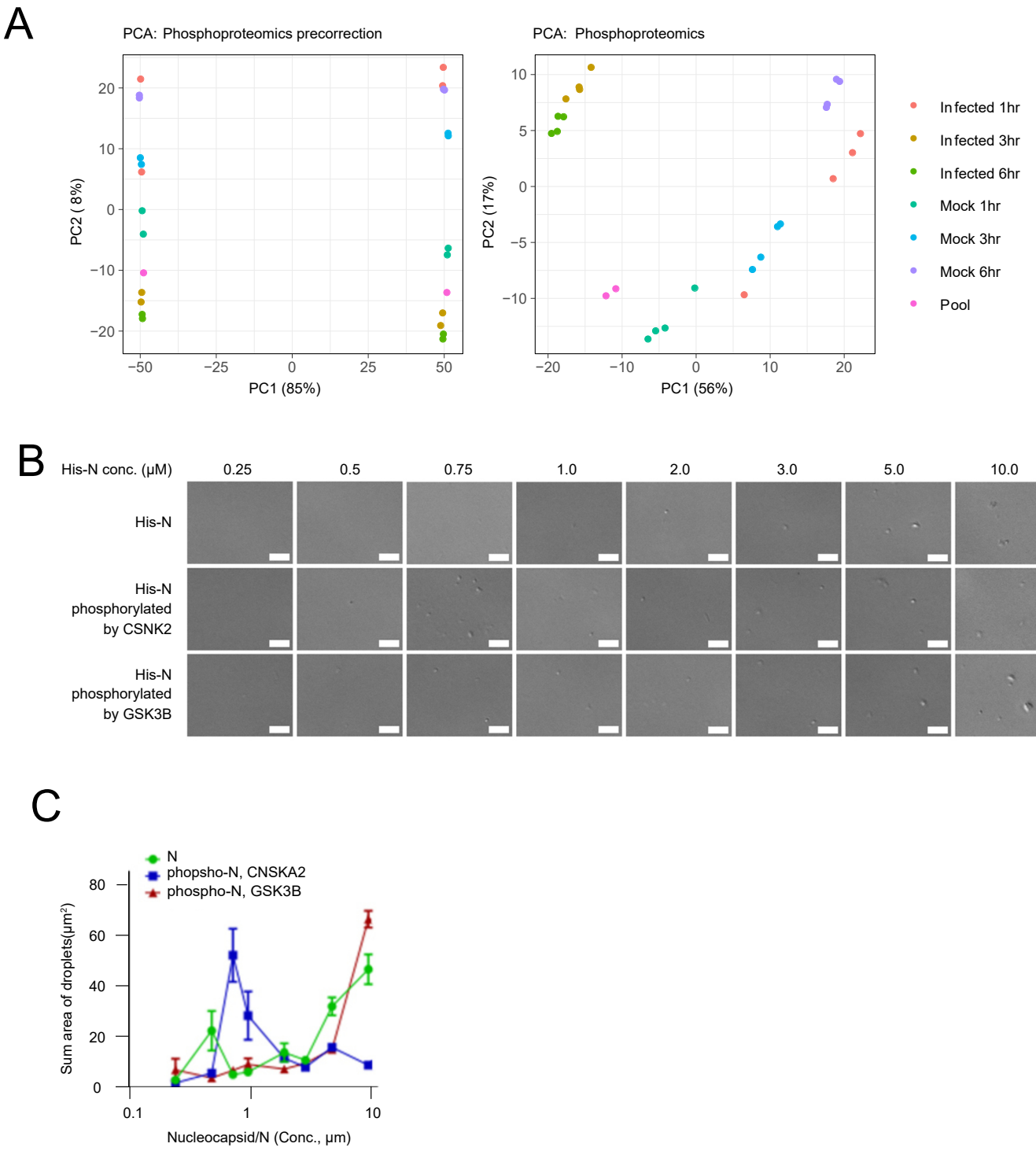

Supplementary Figure S4: PCA clustering of infected iAT2 phosphoproteomic data and phase-separation analysis of SARS-CoV-2 Nucleoprotein (N), Related to Figure 3. (A). Principal component analysis (PCA) of phosphoproteomic site reporter ion intensity for log transformed, normalized data showing pre-batch correction (left) and post-batch correction (right). **(B).** His-N or His-N phosphorylated by CSNK2A2 or GSK3, were used at the concentrations in phase separation reactions and imaged with DIC (differential interference contrast) microscopy at 63x magnification. **(C).** Quantification of number of droplets at various concentrations of recombinant SARS-CoV-2 nucleocapsid either phosphorylated by CSNKA2, GSK3B or not phosphorylated.

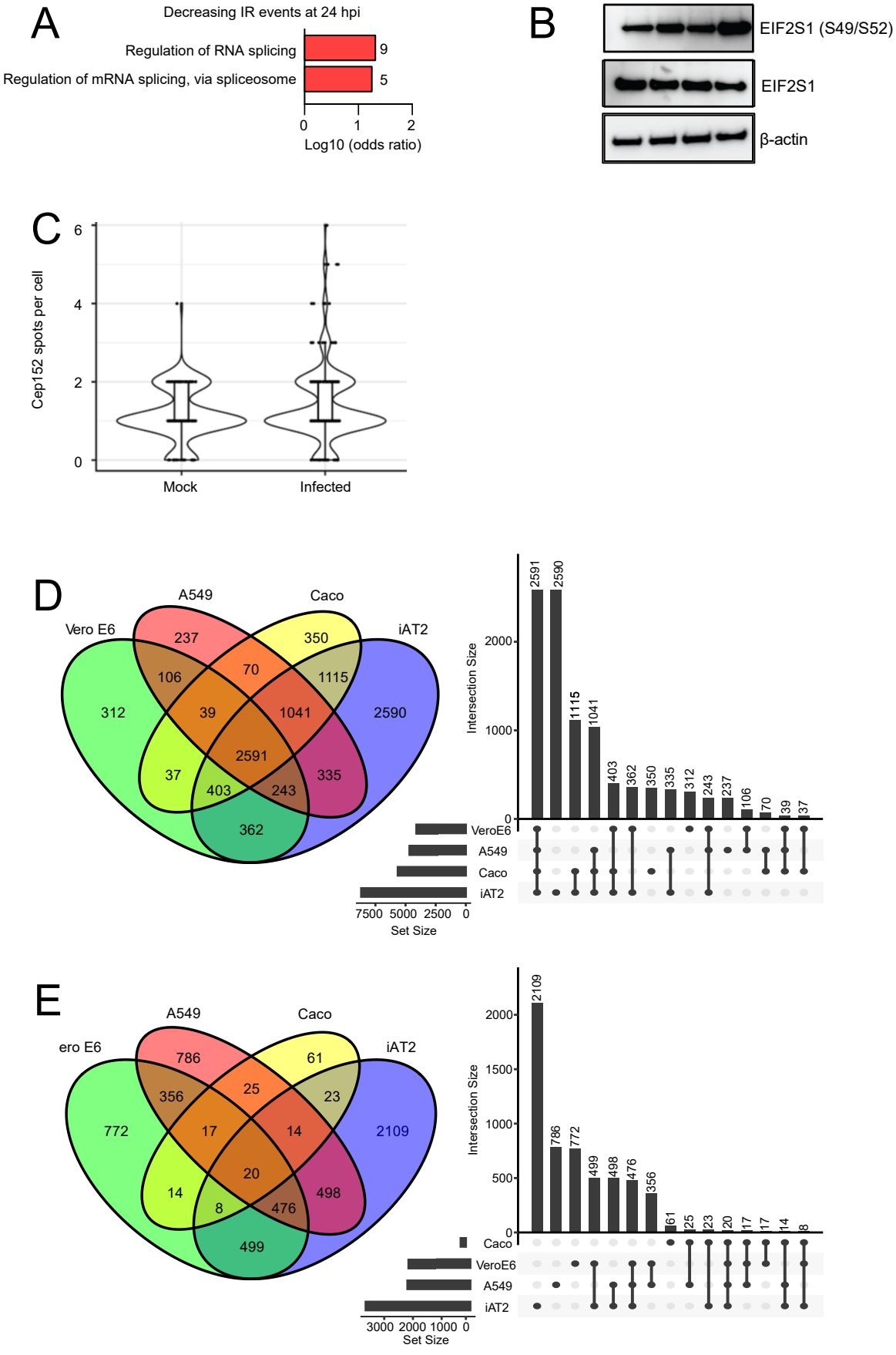

Supplementary Figure S5: Validation of deregulated processes in SARS-CoV-2 infected iAT2s and comparative analysis of present and published SARS-CoV-2 infection datasets, Related to Figure 4 and 5. (A). GO biological enrichment of genes with decreasing intron retention events at 24 hpi based on RNA seq data. **(B).** Immunoblotting analyses of iAT2s mock-infected or infected with SARS-CoV-2 for 24 hours. Lysates were probed with the indicated antibodies. Beta-actin was used as the loading control. **(C).** Violin plot showing centrosomal foci quantified in mock or SARS-CoV-2-infected iAT2s stained with antibodies against CEP152 via immunofluorescence analyses. **(D).** Venn diagram and bar plot showing unique proteins (annotated by respective gene symbols) identified in the Caco-2, VeroE6, A549, and iAT2 cell proteomic studies for SARS-CoV-2 infection. **(E).** Venn diagram and bar plot showing differential (FDR< 0.05, Absolute log fold-change > 0.25) Gene Symbols identified in the Caco-2, VeroE6, A549, and iAT2 cell proteomic studies for SARS-CoV-2 infection.

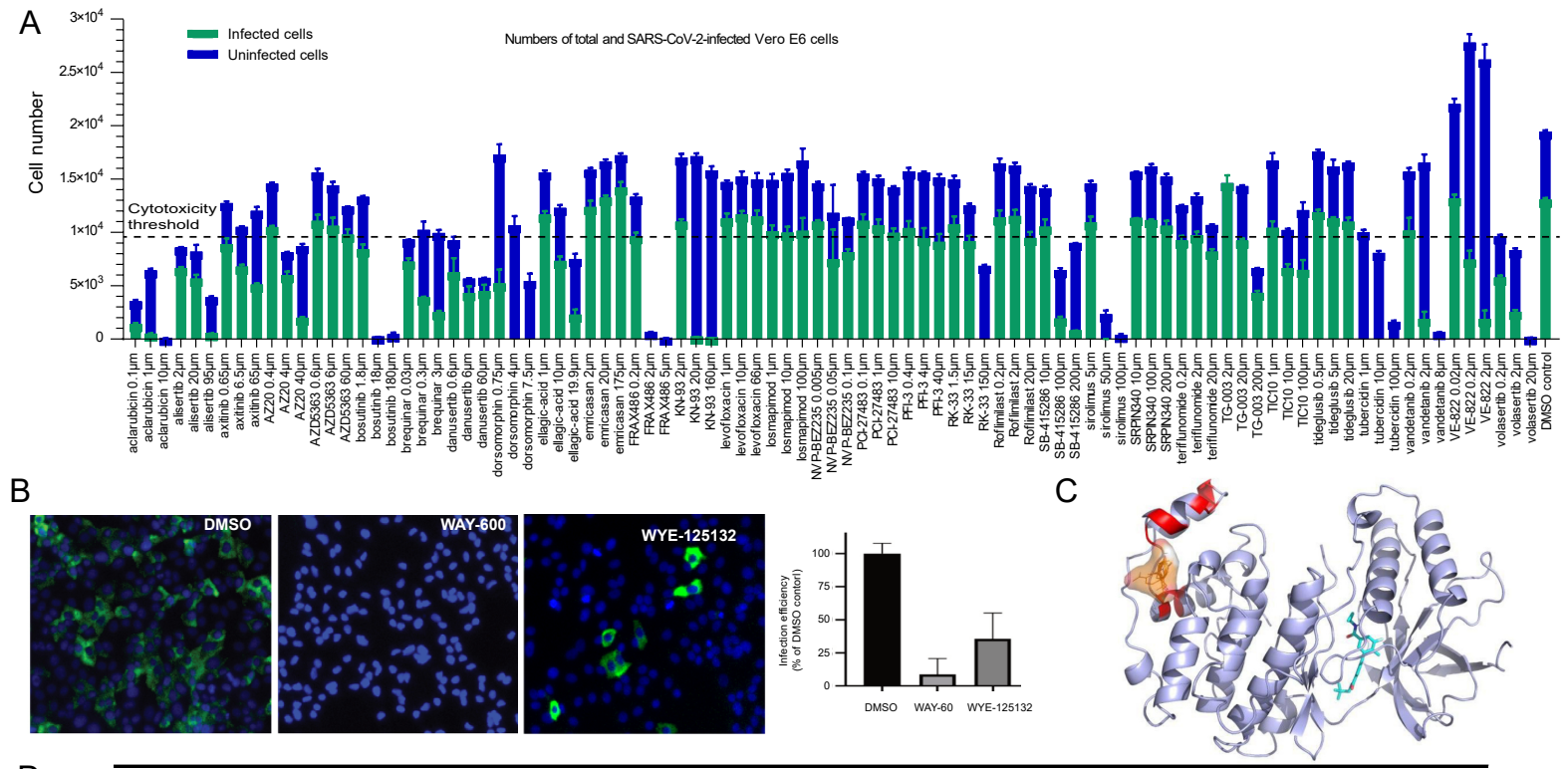

D

Concentration tested (μM) and relative infection rate (IR, in %) in iAT2 cells

Drug name	Clinical status	Relevant target	[μM]	IR	[μM]	IR	[μM]	IR
aclarubicin	Launched	TOP1, TOP2A	50.0	41.4	-	-	-	-
axitinib	Launched	PLK4	0.2	21.0	-	-	-	-
AZ20	Preclinical	ATR, MTOR	0.4	15.1	4.0	8.5	40.0	14.7
AZD5363	Phase 3	AKT1, AKT2, AKT3	120.0	38.9	-	-	-	-
bosutinib	Launched	CAMK2G, CDK2	1.8	65.3	5.4	123.6	16.2	136.0
brequinar	Phase 2	DHODH	0.3	14.8	3.0	44.3	-	-
danusertib	Phase 2	AURKA, AURKB, AURKC	60.0	90.4	-	-	-	-
dorsomorphin	Preclinical	RPS6KA1	4.0	26.9	7.5	29.2	-	-
ellagic-acid	Phase 2	CSNK2A1, GSK3B	19.9	CT	-	-	-	-
emricasan	Phase 2	CASP1, CASP3, CAPS7	175.0	24.0	-	-	-	-
FRAX486	Preclinical	PAK2	0.2	7.1	-	-	-	-
KN-93	Preclinical	CAMK2A, CAMK2G	25.0	17.4	75.0	2.8	150.0	1.7
levofloxacin	Launched	TOP2A	66.0	4.0	-	-	-	-
losmapimod	Phase 3	MAPK14	200.0	7.5	-	-	-	-
NVP-BEZ235	Phase 3	ATR, MTOR	0.2	31.6	-	-	-	-
PCI-27483	Phase 2	ERK1, ERK2	20.0	55.6	-	-	-	-
PFI-3	Preclinical	SMARCA4	40.0	62.8	-	-	-	-
RK-33	Preclinical	DDX3	50.0	168.8	-	-	-	-
Roflumilast	Launched	PDE4	20.0	45.1	-	-	-	-
SB-415286	Preclinical	GSK3B, RPS6KB1	50.0	93.9	100.0	28.1	-	-
SRPIN340	Preclinical	SRPK1, SRPK2	200.0	82.5	-	-	-	-
TIC10	Phase 2	ATKT1, MAPK1	100.0	31.6	-	-	-	-
tubercidin	Phase 1	viral polymerase	10.0	4.3	-	-	-	-
vandetanib	Launched	EGFR, VEGFA	2.0	43.0	8.0	22.2	-	-
VE-822	Phase 2	ATM, ATR, MTOR	2.0	26.8	8.0	155.8	-	-
volasertib	Phase 3	PLK1	0.2	28.7	2.0	30.1	5.0	33.0

Supplementary Figure S6: Drug compound screening of SARS-CoV-2 infected Vero and iAT2 cells, Related to Figure 6. (A). Vero E6 cells were treated with either vehicle (DMSO) or the indicated drugs and respective concentrations. The cells were then immunoprobed with antibodies against SARS-CoV-2 N protein. (B). Expression of N was quantitatively assessed via immunofluorescence analysis, normalized to DMSO control, and presented as +/- s.d. Immunofluorescence analysis of SARS-CoV-2- or mock-infected Vero E6 cells treated with either vehicle (DMSO) or 8 μM of WAY-600 or WYE-125132 and probed with antibodies against SARS-CoV-2 N protein. Cells were counterstained with DAPI and imaged at 20x magnification. Bar plot depicts small-molecule inhibition of viral replication relative to DMSO (Vehicle); cells positive for N staining represented as +/- s.d. **(C)**. Shown here is a simulated 3-D structure of MAPK14 depicting the bound all molecule inhibitor losmapimod (cyan). The region containing mutations (red) in MAPK14 constitute differences between *Homo sapiens* and *Chlorocebus sabaeus*. The region highlighted in orange specifies the location of a putative allosteric binding site in the vicinity of the mutations, as identified by the hotspot identification program FTMap (Yueh et al., 2019, J Med Chem). [Yueh C, Rettenmaier J, Xia B, et al. Kinase Atlas: Druggability Analysis of Potential Allosteric Sites in Kinases. J Med Chem. 2019;62(14):6512-6524. doi:10.1021/acs.jmedchem.9b00089]. **(D)**.Concentration (μM) and relative infection rate (IR, in %) of drugs tested in iAT2 cells.

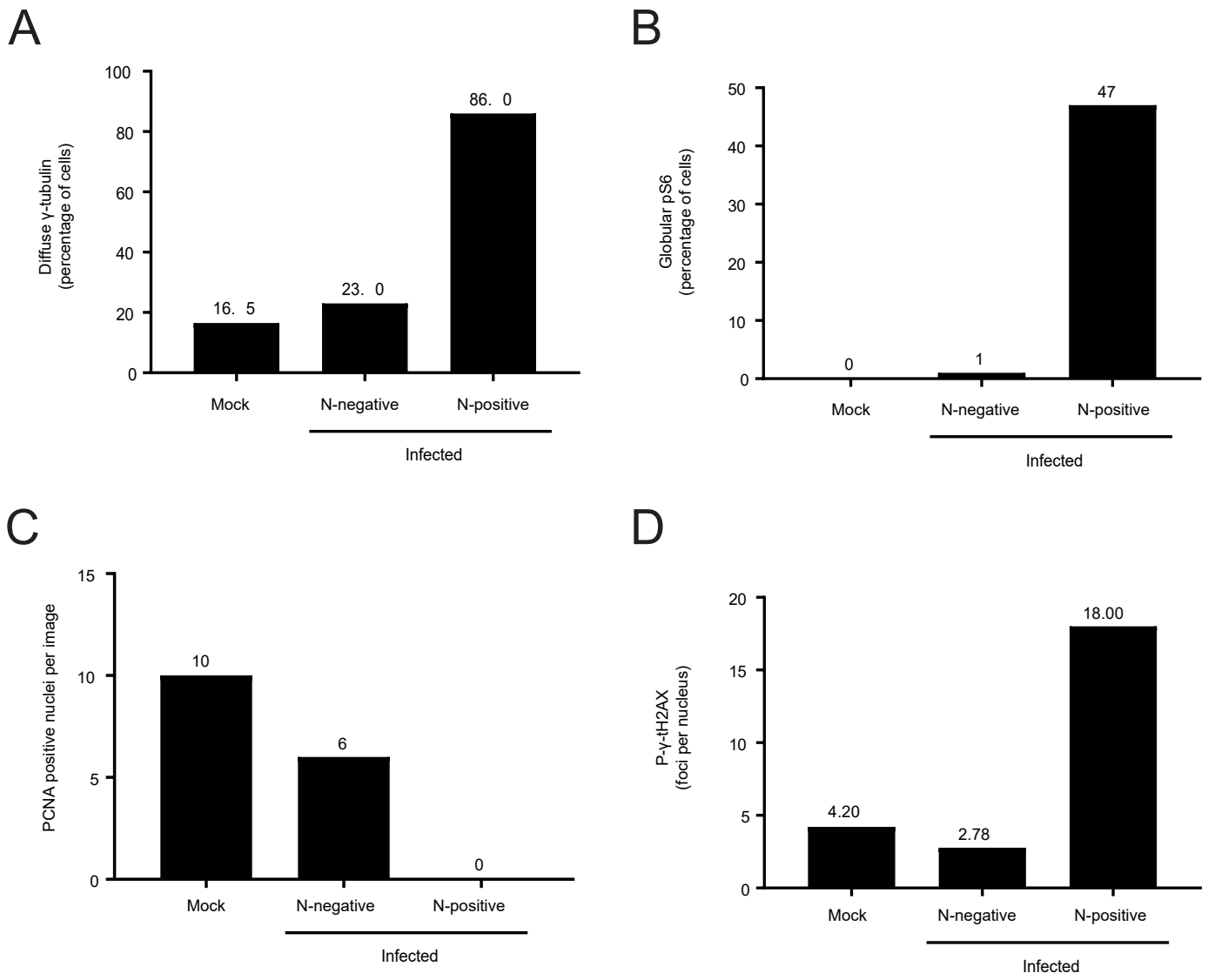

Supplementary Figure S7: SARS-CoV-2 infected iAT2s show deregulated cell cycle, translation and DNA damage responses, Related to Figure 2, 3 and 4. Quantification of immunostained **(A)**. γ-tubulin, **(B)**. pS6, **(C)** PCNA and **(D)**. phospho-γ-H2AX in iAT2 Air Liquid Interface (ALI) cultures that were either mock infected or infected with SARS-CoV-2 at an MOI = 5 for 24 hours. Quantification of SARS-CoV-2 was determined by staining for the SARS-CoV-2 nucleocapsid protein.